BIOCHEMICAL AND BIOPHYSICAL RESEARCH COMMUNICATIONS **219,** 205–212 (1996)
ARTICLE NO. 0206

NMR-Based, Molecular Dynamics- and Random Walk Molecular Mechanics-Supported Study of Conformational Aspects of a Carbohydrate Ligand (Galβ1-2Galβ1-R) for an Animal Galectin in the Free and in the Bound State

Hans-Christian Siebert,*,† Martine Gilleron,†,‡ Herbert Kaltner,* Claus-Wilhelm von der Lieth,§ Tibor Kozár,§,¶ Nicolai Bovin,‖ Elena Y. Korchagina,‖ Johannes F. G. Vliegenthart,† and Hans-Joachim Gabius*,[1]

**Institut für Physiologische Chemie, Tierärztliche Fakultät, Ludwig-Maximilians-Universität, Veterinärstraße 13, D-80539 München, Germany; †Bijvoet Center for Biomolecular Research, Department of Bio-Organic Chemistry, Utrecht University, P.O. Box 80.075, NL-3508 TB Utrecht, The Netherlands; ‡CNRS, Laboratoire de Pharmacologie et de Toxicologie Fondamentale, Départment III: Glycoconjugués et Biomembranes, 118, Route de Narbonne, F-31062 Toulouse, Cédex, France; §Deutsches Krebsforschungszentrum, Zentrale Spektroskopie, Im Neuenheimer Feld 280, D-69120 Heidelberg, Germany; ¶Slovak Academy of Sciences, Institute of Experimental Physics, Department of Biophysics, 04353 Kosice, Slovakia; and ‖Shemyakin Institute of Bioorganic Chemistry, Russian Academy of Sciences, ul. Miklukho-Maklaya, 16/10, Moscow, Russian Federation*

Received December 12, 1995

The binding of a carbohydrate to a lectin may affect the conformation of the ligand. To address this question for the galectin from chicken liver, the conformation of Galβ1-2Galβ1-R was analyzed in the free and in the galectin-bound state with 2D-ROESY- and 1D- as well as 2D-transferred NOE-experiments. A computer-assisted analysis of spatial parameters of the ligand by molecular dynamics (MD) and random walk molecular mechanics (RAMM) calculations, taking different dielectric constants from $\epsilon = 1$ to $\epsilon = 80$ and various force fields into account, were instrumental to define the energetic minima of the free state. NMR-derived interresidual distance constraints enabled a conformational mapping. The two overlapping interresidual distance constraints obtained from transferred-NOE experiments of the galectin-ligand complex clearly support the notion that the conformation of the disaccharide in the bound state is at least very close to its global energy minimum state in solution.

Protein-carbohydrate interactions can guide crucial physiological reactions such as cell adhesion, inter- and intracellular glycoprotein routing and regulation of various cellular functions (1, 2). Their evident importance prompts to analyze in detail the molecular characteristics of this type of recognition in solution. The combination of computer-assisted calculations of the conformation and NMR-based experiments for the free ligand and lectin-saccharide complex provides a suitable tool to address this question. It enables us to compare spatial parameters of a certain ligand before and after association with members of a lectin family with similar binding specificity, e.g. to galactosides. Agglutinins of this class mediate cell-matrix interactions and enhance immune functions (3–5). Due to the remarkable affinity of Galβ1-2Galβ1-R to the immunomodulatory *Viscum album* agglutinin, reported previously (6, 7), we have chosen to map conformational aspects of this high-affinity ligand for galactoside-binding lectins of organisms from different branches of the evolutionary tree. Herein, we report the first study in this area for an animal galectin. Transferred nuclear Overhauser effect (TRNOE)-based experiments in combination with conformational distance mapping, random walk molecular mechanics (RAMM) and molecular dynamics (MD) calculations indicate that the actual conformations of this disaccharide in the complex and in the free form are at least very similar.

[1] To whom correspondence should be addressed.

0006-291X/96 $18.00

MATERIALS AND METHODS

Preparation of the ligand. A mixture of 1-O-[3′-(trifluoroacetamido)propyl]-3-O-acetyl-4,6-O-benzylidene-β-D-galactopyranoside (200 mg, 0.43 mmol), prepared as described (8), mercuric cyanide (218 mg, 0.86 mmol), mercuric bromide (30 mg, 0.89 mmol), and molecular sieves with size limit of 4 Å (2 g) in dry dichloromethane was stirred for 2 h under a nitrogen atmosphere. Additional molecular sieve material (1 g) and 2,3,4,6-tetra-O-benzyl-α-D-galactopyranosyl bromide (510 mg, 0.86 mmol) in 5 ml of dichloromethane were then added, and the mixture was kept for 20 h at room temperature with gentle stirring. Thereafter, it was diluted with chloroform, and the organic layer was washed successively with water, 5% potassium iodide solution, and water, dried with sodium sulfate and evaporated in vacuo. Column chromatography (2 × 15 cm) on Silica Gel 40–100 μm (CSFR) (hexane/ethylacetate, 20–100% of ethylacetate) of the residue gave protected Gal′β1-2Galβ1-Osp (70 mg, 16%) with a Rf-value of 0.5 in thin layer chromatography (hexane/ethylacetate, 1:1) and protected Gal′α1-2Galβ1-Osp (300 mg, 80%). The denoted residue refers to the non-reducing end. Osp is the abbreviation of -$OCH_2CH_2CH_2NHCOCF_3$. The ββ′-disaccharide compound was deprotected by successive de-O-acetylation (MeONa/MeOH), acid hydrolysis (70% AcOH) at 80°C for 15 min and hydrogenolysis (10% Pd/C), and yielded Gal′β1-2Galβ1-Osp in 69%, $[\alpha]_D$ +4° (*c* 0.6, H_2O).

Isolation of the galectin. The β-galactoside-binding lectin from chicken liver was purified by successive application of affinity and ion-exchange chromatography. The homogeneity was ascertained by two-dimensional gel electrophoresis, as described (9, 10).

Computer-assisted calculations. The calculations were performed on Silicon Graphics workstations. Several molecular dynamics (MD) trajectories were calculated with the DISCOVER software using different parametrizations: CVFF (*C*onsistent *V*alence *F*orce *F*ield) (11, 12) and the AMBER program (*A*ssisted *M*odel *B*uilding with *E*nergy *R*efinement) (13, 14). In addition, other programs with different force fields, e.g. CHEAT (*C*arbohydrate *H*ydroxyls represented by *E*xtended *AT*oms) (15), CHARMM (*C*hemistry at *HAR*vard *M*acromolecular *M*echanics) (16), and GROMOS (*GRO*ningen *MOL*-lecular *S*imulations) (17) have been tested to predict conformational preferences of Gal′β1-2Galβ1-Osp. The input files for molecular dynamics simulations (DISCOVER V.2.95 program of Biosym Technologies, San Diego, USA) were prepared following the automatic charge and parameter assignment procedure of INSIGHTII (V.2.5, Biosym Technologies, San Diego, USA). Dihedral angles ϕ and ψ are defined as follows:

ϕ: H1′-C1′-O1′-CX; ψ: C1′-O1′-CX-HX. ϕ corresponds to ϕ_H, ψ corresponds to ψ_H according to the IUPAC conventions. A (ϕ/ψ) combination of (+/−180°/0°) is defined as anti-conformation, because the two protons are in an anti- or trans-position. A (ϕ/ψ) combination of (0°/0°) is defined as cis-conformation, because the two protons are in a cis-or syn-position.

With the help of a molecular mechanics (MM) grid search using the RAMM program (18) the possible local energy minima defined by the glycosidic angles were determined in the conformational space of Gal′β1-2Galβ1-Osp. In MM calculations a stepwise change of the glycosidic torsion angles ϕ, ψ in combination with energy minimization at each step was performed. Moreover, for each combination of the ϕ, ψ torsional angles different orientations of the hydroxyl and hydroxymethyl-groups were generated by the random walk technique to turn these side groups, too, into the lowest-energy position. The RAMM program is especially suitable to detect local minima of higher energy than those which are normally adopted in a molecular dynamics run (19). The force field and energy functions used in RAMM correspond to the Allinger molecular mechanics method MM2-87 (20, 21).

NMR measurements and distance mapping. 500 MHz ^{1}H-NMR spectra were recorded on a Bruker AM 500 spectrometer. Prior to ^{1}H-NMR spectroscopy, the disaccharide and lectin preparations were repeatedly dissolved in D_2O and lyophilized, finally using D_2O (99.96 atom %, Merck, Sharp and Dohme, Montreal, Canada) at p^{2}D 7. Assignment of the chemical shifts was carried out by standard NMR experiments like COSY (*CO*rrelated *S*pectroscopy*Y*) and TOCSY (*TO*tal *C*orrelated *S*pectroscopy*Y*). 2D-ROESY (*R*otating Frame *O*verhauser *E*ffect *S*pectroscop*Y*) (22, 23) and 1D- and 2D-TRNOE (*TR*ansferred *N*uclear *O*verhauser *E*ffect) measurements (24–27) were used for determination of conformational parameters of the ligand in the free and in the galectin-bound state. The mixing times for ROESY and TRNOE experiments were set to 50, 100, 200 and 300 ms. NOE constraints in the free and in the bound state were evaluated using the distance mapping procedure (28–30). For the conformational analysis of the glycosidic linkage the Ramachandran-type representation was used, where distance constraints for each atom pair are expressed in the form of their ϕ, ψ coordinates. Contours drawn for the determined values and also lower and upper limits of the possible distance of one NOE contact still enclose a large number of ϕ, ψ combinations and, thus, do not define any particular conformation. If, however, this region overlaps with another region defined by a second NOE contact, the probable conformational space is reduced, limiting the number of combinations for the glycosidic angles ϕ, ψ.

RESULTS AND DISCUSSION

As a first step in our study the conformation of the disaccharide was analyzed by molecular dynamics calculations with increasing dielectric constants or explicit inclusion of water in various force fields, as exemplarily illustrated for MD simulations of Gal′β1-2Galβ1-R with dielectric constants of $\epsilon = 1$ and $\epsilon = 80$ in Fig. 1a,b. The force field, which has been used for these

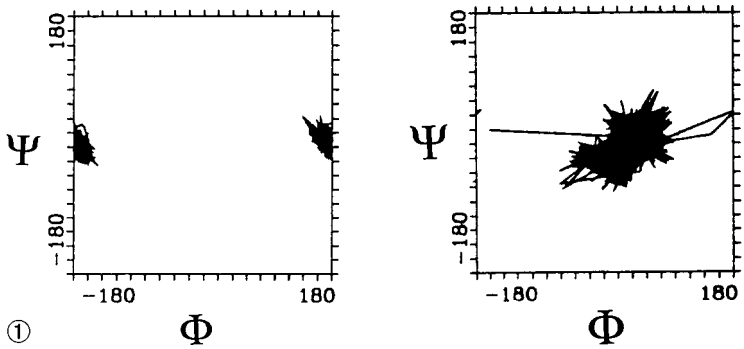

FIG. 1. RAMM conformational energy map of Gal′β1-2Galβ1-R at different values of the dielectric constant, namely $\epsilon = 1.5$ (a) and $\epsilon = 4$ (b).

calculations, is CVFF (15, 16). In each case, the initial structure is the anti-conformer, which corresponds to the local side-minimum calculated by RAMM, as shown in Fig. 1a,b. In the case of the low dielectric constant Gal′β1-2Galβ1-Osp remains in its anti-conformational state, whereas a rather broad minimum near the cis-position including a combination of angles of about $\phi = 25°$ and $\psi = -50°$ is adopted immediately, when the dielectric constant of aqueous solution is employed. This result suggests that the actual free-state conformation in solution may resemble this spatial arrangement.

RAMM calculations were used to analyze the energy profile of Gal′β1-2Galβ1-R in detail. Remarkable changes in the energy profile can be seen when the dielectric constant of $\epsilon = 1.5$ is changed to a value of $\epsilon = 4$ (Fig. 2a,b). It is indeed notable that a so-called trans- or anti-conformation including $\phi = -180°$ and $\psi = 0°$ has a low energy minimum comparable to the level of that in the cis-position (Fig. 2a). Hence, the disaccharide may adopt an anti-conformation in the free state, which has recently been described as a possible solution conformation for disaccharides (31). A distinct parameter which should be varied in the setting of such calculations is the dielectric constant. As already revealed by the MD runs, a change of the dielectric constant from 1.5 to 4 leads to a favorable cis-conformation (Fig. 2b). Such deliberate changes may reveal energetically suitable and thus adoptable conformers with relevance for complex formation. It should also not be neglected that the dielectric constant of the immediate binding pocket may well deviate from the

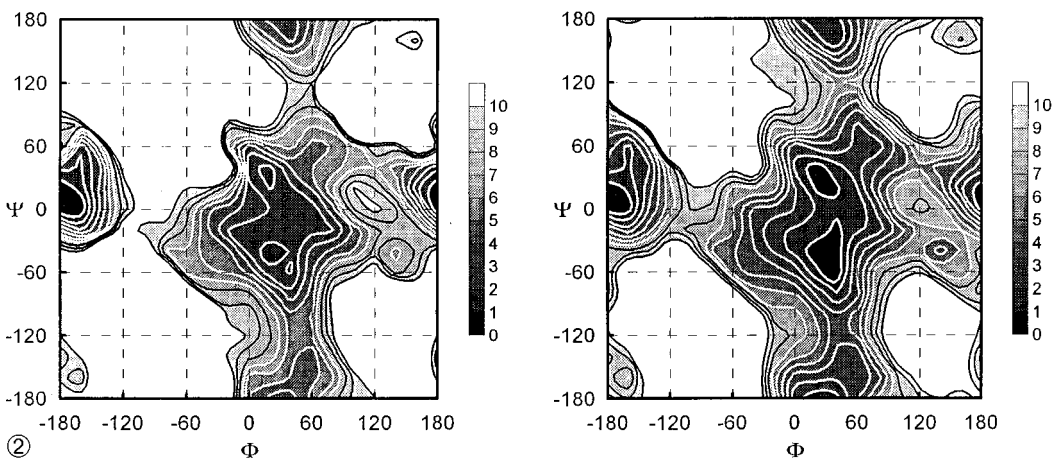

FIG. 2. Representation of the conformational behavior of Gal′β1-2Gal′β1-R in a MD simulation using CVFF with dielectric constants at $\epsilon = 1$ (a) and $\epsilon = 80$ (b), respectively.

value of the aqueous medium. Since the energy values of the anti-conformer of Gal′β1-2Galβ1-R are enhanced with increasing values of the dielectric constant, as demonstrated in Fig. 2a,b, only the two energetic minima near the cis-position can be predicted to be strongly populated under this condition (Fig. 2b).

Experimentally, NMR measurements are instrumental to support this assumption. Results of ROESY-experiments of free Gal′β1-2Galβ1-Osp enabled us to determine an interresidual distance of 2.75 Å between Gal′ H1 and Gal H2, using the intraresidual distance between Gal H1-Gal H3 of 2.6 Å for calibration (Fig. 3). The intensity of the cross-peak of the two anomeric protons Gal′ H1 and Gal H1 in the ROESY-spectrum corresponds to a distance of 3.35 Å. The two interresidual proton contacts measured for Gal′β1-2Galβ1-Osp are in agreement with a conformation, which is established by values for the glycosidic angles of $\phi = 20°$ and $\psi = -60°$. The Osp group of the Gal′β1-2Galβ-derivative has no influence on the conformation of the disaccharide when compared with the reducing disaccharide Gal′β1-2Gal (not shown).

Having provided evidence for the actual free state conformation, further NMR experiments were aimed to determine such structural aspects of the ligand after complex formation. Herein, the molar fractions of bound and free ligand must be adjusted adequately to maximize strong negative NOEs, measureable from the complex. With a 10–20fold molar excess of carbohydrate no significant differences in the quality of the TRNOE-data were apparent. In principle, three conditions which ensure a meaningful study were fulfilled in the TRNOE-experiments: (I) the negative NOE signals of the bound ligand were predominant relative to the NOE signals of the free ligand, as achieved by appropriate adjustment of the relation of ligand to lectin, (II) the effects of spin diffusion were minimized by testing several mixing times (50 ms–300 ms), and (III) it was possible to exclude signals, originating from protein-protein interactions, by recording a reference spectrum. This reference spectrum was obtained by irradiation with a resonance frequency of a part of the spectrum where only protein signals occur in the case of 1D-TRNOE-experiments. In the case of 2D-TRNOE-experiments, spectra of the ligand-free lectin and the lectin-free ligand were recorded.

The 1D ^{1}H-NMR spectrum of the animal galectin at a millimolar concentration displayed fairly broad and unresolved signals. Therefore, irradiation at the frequency of distinct saccharide signals was possible in 1D-TRNOE experiments of (Gal′β1-2Galβ1-Osp)-galectin complexes. Overall, the results obtained from concomitant 2D-TRNOE-experiments were in agreement with those from 1D-TRNOE experiments. The relevant part of a 2D-TRNOE spectrum is shown in Fig. 4. The distance between Gal′ H1 and Gal H2 was ascertained to be 2.7 Å by using the intensities of the intraresidual proton-proton cross-signals of Gal H1 and Gal H3, with an interproton distance of 2.6 Å for calibration. The distance of 3.3 Å between Gal′ H1 and Gal H1 was measured using the same calibration. The cross-peak of Gal′ H1 and Gal H3, marked with a ''*'', arises due to spin-diffusion effects. The measured distances have to be considered as virtual due to molecular flexibility. The distance constraint Gal′ H1-Gal H2 with an averaged distance of 2.7 Å is plotted in the distance

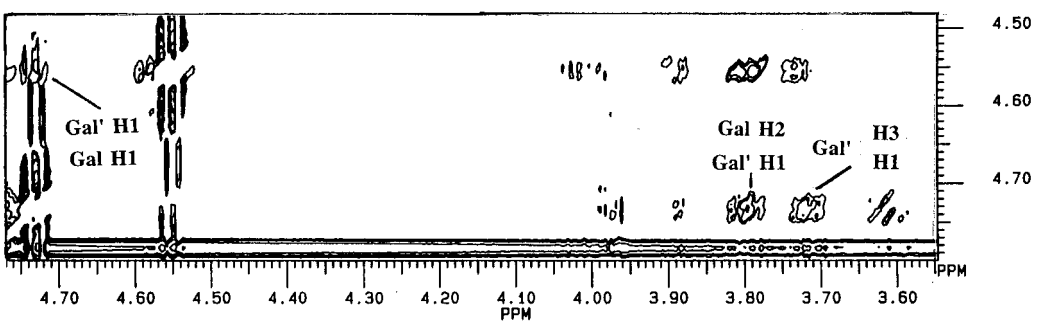

FIG. 3. Relevant part of a 2D-ROESY spectrum of Gal′β1-2Gal′β1-Osp.

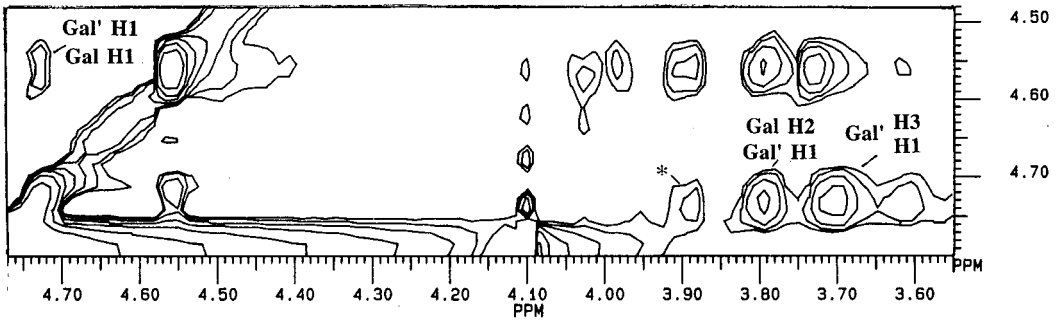

FIG. 4. Relevant part of a 2D-TRNOE spectrum of the Gal′β1-2Gal′β1-Osp—galectin, complex.

map representing the conformational space of the glycosidic angles (ϕ/ψ) of galectin-bound Gal′β1-2Galβ1-R. The second interresidual distance constraint Gal′ H1-Gal H1 of 3.3 Å is similarly added. The contour lines of these constraints overlap in a distinct area of the distance map, as can be seen in Fig. 5. This region, which is defined by experimental data, is indicative for real conformations of the bound ligand. A positive ψ-value, as predicted from Fig. 2b, does not lie in this region of overlap.

The results of the NMR-experiments and the computational calculations of Gal′β1-2Galβ1-R

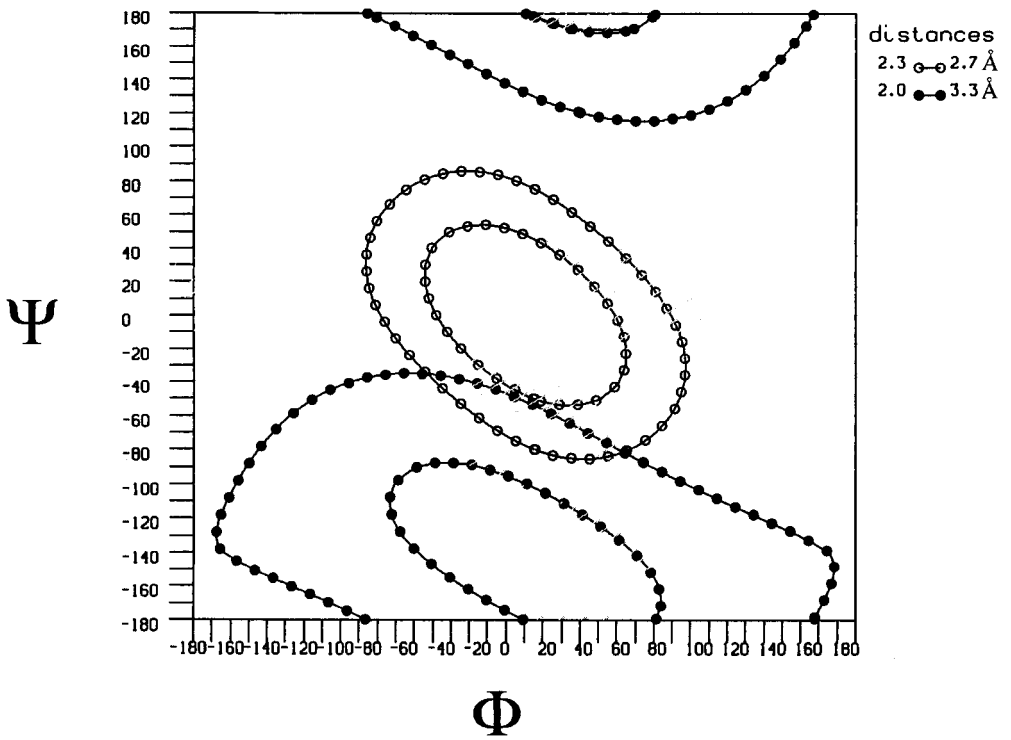

FIG. 5. Distance map of Gal′β1-2Gal′β1-R with two interresidual NOE contacts in complex state. The measured interresidual contact of 2.7 Å between Gal′ H1 and Gal H2 corresponds to a defined contour line (&hb9;-&hb9;) in the ϕ, ψ diagram. The measured interresidual contact of 3.3 Å between Gal′ H1 and Gal H1 accounts for a second contour line (&sb9;-&sb9;). These two lines define a region of overlap indicating permissible sets of ϕ, ψ-values. The lower limits, given as a second set of contour lines, are defined, e.g., by the van der Waals distance. The hatched area shows the geometrically allowed region when the disaccharide is considered to be rigid except for the glycosidic linkage.

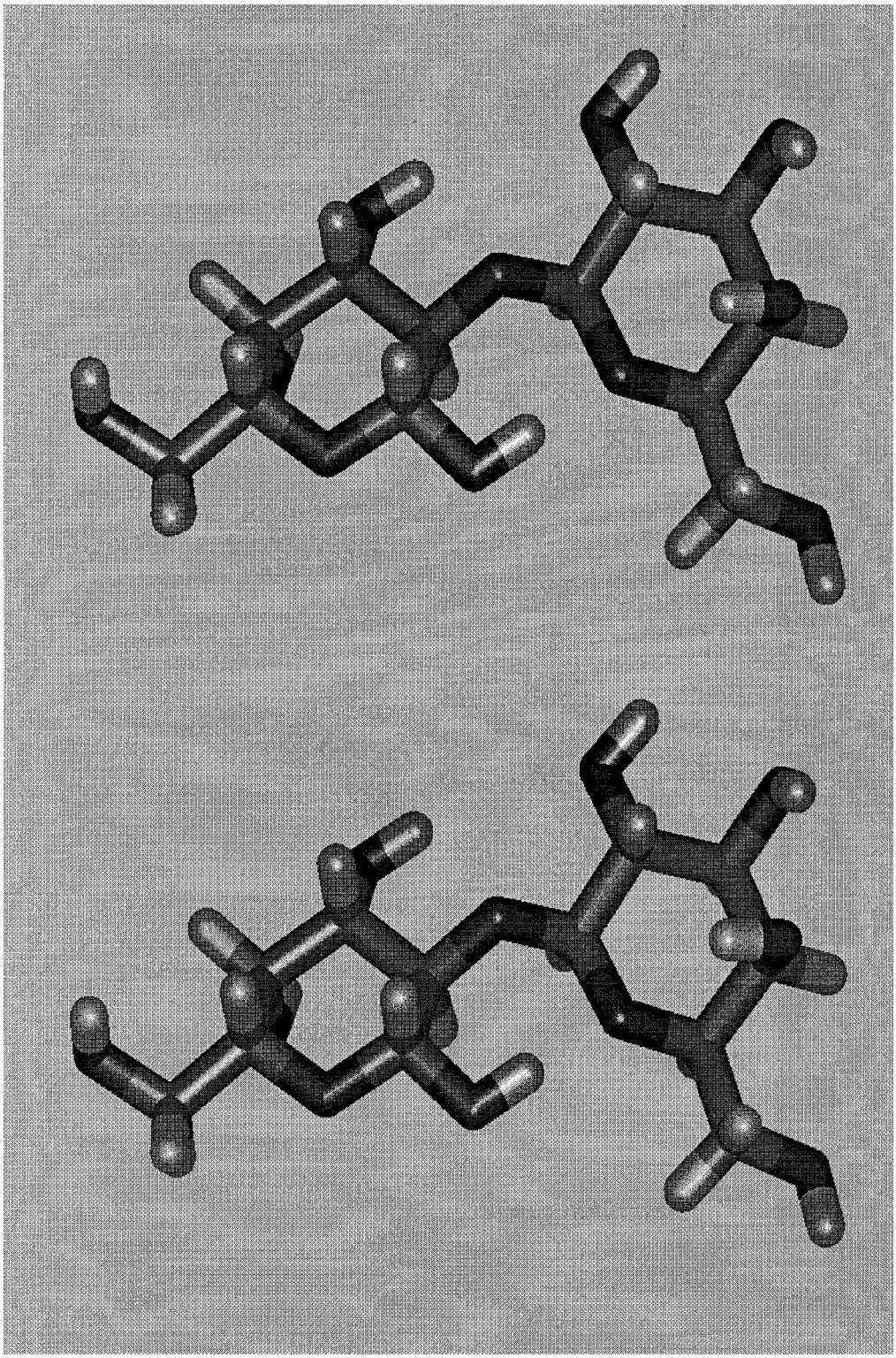

FIG. 6. Stereo plot representation of the most probable conformation of the disaccharide ligand Gal′β1-2Gal′β1-R in the complex.

are consistent with the assumption that the conformation of the bound ligand in solution can adopt a conformation, which is at least similar to that of a global energetic minimum in the absence of the lectin (Fig. 6). This combined NMR- and computational study of Gal′β1-2Galβ1-R underscores that the different functional groups of the ligand are apparently already in a position which allows the lectin to bind this energetically favorable conformer.

The present state of NMR-based analysis of galactose-containing ligand-antibody/lectin-complexes precludes a definitive conclusion on the relation of free- to bound-state ligand conformation in this specificity class of saccharide receptors (32–36). X-ray structures of bacterial toxins and a mammalian galectin indicate that the torsion angles at the glycosidic linkage of a bound galactose moiety in the crystal lattices are similar to those regions of low energy positions in solution (37–40). Knowledge about the actually bound conformation will be pivotal to devise high-affinity ligands especially for clinically relevant lectins to block access to them or target drugs (41–43). Even in the absence of a complete X-ray analysis for a lectin under investigation, docking studies can be performed with the help of available data on related agglutinins (44), as currently performed. Distinct predictions of such a modeling approach are being experimentally tested for the parameter of surface accessibility of tryptophan, tyrosine and histidine residues by the laser photo CIDNP (chemically induced dynamic nuclear polarization) technique (Siebert et al., in preparation), as recently applied to serum amyloid P component (45).

ACKNOWLEDGMENTS

This investigation was supported by the Human Capital and Mobility Program of the European Community, the Dr.-M.-Scheel-Stiftung für Krebsforschung, the Deutsche Forschungs Gemeinschaft (DFG) and by the Netherlands Foundation for Chemical Research (SON). We sincerely thank Prof. Dr. Janusz Dabrowski from the Max-Planck-Institut für Medizinische Forschung in Heidelberg for valuable help and many fruitful discussions Prof. Dr. Dr. Heinz Staab, head of the Department of Organic Chemistry at the Max-Planck-Institut für Medizinische Forschung, for valuable access to the 500 MHz-NMR spectrometer and Prof Dr. J. Wittmann and Dr. G. Reuter for careful review of the manuscript.

REFERENCES

1. Gabius, H.-J. (1991) *Biochim. Biophys. Acta* **1071,** 1–18.
2. Gabius, H.-J., and Gabius, S., (Eds.) (1993) Lectins and Glycobiology, Springer Publ. Co., Heidelberg–New York.
3. Hirabayashi, J., and Kasai, K. (1993) *Glycobiology* **3,** 297–304.
4. Gabius, H.-J. (1994) *Trends Glycosci. Glycotechnol.* **6,** 229–238.
5. Barondes, S. H., Cooper, D. N. W., Gitt, M. A., and Leffler, H. (1994) *J. Biol. Chem.* **269,** 20807–20810.
6. Lee, R. T., Gabius, H.-J., and Lee, Y. C. (1992) *J. Biol. Chem.* **267,** 23722–23727.
7. Lee, R. T., Gabius, H.-J., and Lee, Y. C. (1994) *Carbohydr. Res.* **254,** 269–276.
8. Korchagina, E. Y., and Bovin, N. V. (1992) *Bioorg. Khim.* **18,** 283–298.
9. Beyer, E. C., Zweig, S. E., and Barondes, S. H. (1980) *J. Biol. Chem.* **255,** 4236–4239.
10. Schneller, M., André, S., Cihak, J., Kaltner, H., Merkle, H., Rademaker, G. J., Haverkamp, J., Thomas-Oates, J., Lösch, U., and Gabius, H.-J. (1995) *Cell. Immunol.* **166,** 35–43.
11. Hagler, A. T., Huler, E., and Lifson, S. (1974) *J. Am. Chem. Soc.* **96,** 5319–5327.
12. Hagler, A. T., Lifson, S., and Dauber, P. (1979) *J. Am. Chem. Soc.* **101,** 5122–5130.
13. Weiner, S. J., Kollman, P. A., Case, D. A., Singh, U. C., Ghio, C., Alagona, G., Profeta Jr., S., and Weiner, P. (1984) *J. Am. Chem. Soc.* **106,** 765–784.
14. Weiner, S. J., Kollman, P. A., Nguyen, D. T., and Case, D. A. (1986) *J. Comput. Chem.* **7,** 230–252.
15. Grootenhuis, P. D. J., and Haasnoot, C. A. G. (1993) *Mol. Sim.* **10,** 75–95.
16. Brooks, R. B., Bruccoleri, R. E., Olafson, B. D., States, D. J., Swaminathan, S., and Karplus, M. (1983) *J. Comput. Chem.* **4,** 187–217.
17. van Gunsteren, W. F. (1988) *Protein Engineering* **2,** 5–13.
18. Kozár, T., Petrak, F., Galova, S., and Tvaroska, I. (1990) *Carbohydr. Res.* **204,** 27–36.
19. von der Lieth, C.-W., Kozár, T., and Hull, W. E. (1995) *J. Mol. Struct.*, in press.
20. Allinger, N. L. (1987) *J. Am. Chem. Soc.* **99,** 8127–8134.
21. Allinger, N. L., Kok, R. A., and Imam, M. R. (1988) *J. Comput. Chem.* **9,** 591–595.
22. Bothner-By, A. A., Stephens, R. L., Lee, J.-M., Warren, C. D., and Jeanloz, R. W. (1984) *J. Am. Chem. Soc.* **106,** 811–813.
23. Bax, A., and Davis, D. G. (1985) *J. Magn. Reson.* **63,** 207–213.

24. Albrand, J. P., Birdsall, B., Feeney, J., Roberts, G. C. K., and Burgen, A. S. V. (1979) *Int. J. Biol. Macromol.* **1,** 37–41.
25. Clore, G. M., and Gronenborn, A. M. (1982) *J. Magn. Reson.* **48,** 402–417.
26. Clore, G. M., and Gronenborn, A. M. (1983) *J. Magn. Reson.* **53,** 423–442.
27. Otting, G. (1993) *Curr. Opinion Struct. Biol.* **3,** 760–768.
28. von der Lieth, C.-W., Schmitz, M., Poppe, L., Hauck, M., and Dabrowski, J. (1989) *in* Softwareentwicklung in der Chemie 3 (Gauglitz, G., Ed.), pp. 371–378, Springer Publ. Co., Heidelberg–New York.
29. Poppe, L., von der Lieth, C.-W., and Dabrowski, J. (1990) *J. Am. Chem. Soc.* **112,** 7762–7771.
30. Siebert, H.-C., Reuter, G., Schauer, R., von der Lieth, C.-W., and Dabrowski, J. (1992) *Biochemistry* **31,** 6962–6971.
31. Dabrowski, J., Kozár, T., Grosskurth, H., and Nifant'ev, N. E. (1995) *J. Am. Chem. Soc.* **117,** 5534–5539.
32. Bevilacqua, V. L., Thomson, D. S., and Prestegard, J. H. (1990) *Biochemistry* **29,** 5529–5537.
33. Glaudemans, C. P. J., Lerner, L., Daves Jr., G. D., Kovác, P., Venable, R., and Bax, A. (1990) *Biochemistry* **29,** 10906–10911.
34. Bevilacqua, V. L., Kim, Y., and Prestegard, J. H. (1992) *Biochemistry* **31,** 9339–9349.
35. Imberty, A., Bourne, Y., Cambillau, C., Rougé, P., and Perez, S. (1993) *Adv. Biophys. Chem.* **3,** 71–117.
36. Bundle, D. R., Baumann, H., Brisson, J.-R., Gagné, S. M., Zdanov, A., and Cygler, M. (1994) *Biochemistry* **33,** 5183–5192.
37. Bourne, Y., Bolgiano, B., Liao, D., Strecker, G., Cantau, P., Herzberg, O., Feizi, T., and Cambillau, C. (1994) *Nature Struct. Biol.*1 **,** 863–869.
38. Liao, D., Kapadia, G., Ahmed, H., Vasta, G., and Herzberg, O. (1994) *Proc. Natl. Acad. Sci. USA* **91,** 1428–1432.
39. Meritt, E. A., Sarfaty, S., van den Akker, F., L'hoir, C., Martial, J. A., and Hol, W. G. J. (1994) *Protein Sci.* **3,** 166–175.
40. Stein, P. E., Boodhoo, A.,, Armstrong, G. D., Heerze, L. D., Cockle, S. A., Klein, M. H., and Read, R. J. (1994) *Nature Struct. Biol.* **1,** 591–596.
41. Gabius, H.-J. (1987) *Cancer Investig.* **5,** 39–46.
42. Bovin, N. V., and Gabius, H.-J. (1995) *Chem. Soc. Rev.*, in press.
43. Gabius, H.-J., Kayser, K., and Gabius, S. (1995) *Naturwissenschaften*, in press.
44. Rini, J. M. (1995) *Ann. Rev. Biophys. Biomol. Struct.* **24,** 551–577.
45. Siebert, H.-C., André, S., Reuter, G., Gabius, H.-J., Kaptein, R., and Vliegenthart, J. F. G. (1995) *FEBS Lett.* **371,** 13–16.